

DOI: 10.1002/cctc.201402018

Nitrogen-Doped Pitch-Based Spherical Active Carbon as a Nonmetal Catalyst for Acetylene Hydrochlorination

Xugen Wang,^[a, b] Bin Dai,^{*[b]} Yang Wang,^[b] and Feng Yu^[b]

A highly active nitrogen-doped pitch-based spherical activated carbon catalyst (PSAC-N) is synthesized through a nitrogen-doping treatment and used as a nonmetal catalyst for acetylene hydrochlorination. The conversion of acetylene on PSAC-N exceeds 68% and the selectivity of vinyl chloride is over 99% at a temperature of 250 °C, an acetylene gas hourly space velocity of 120 h⁻¹, and a feed volume ratio $V(\text{HCl})/V(\text{C}_2\text{H}_2)$ of 1.15. DFT calculations performed with Gaussian 09 program package reveal that the active site of PSAC-N has a N-6v (qua-

ternary nitrogen bonded between two 6-membered rings) structure. A seven benzene ring unit model is used in the DFT study. In addition, the reason for inactivation for PSAC-N catalysts is discussed. Of all the adsorption energies obtained, the adsorption capacity of hydrogen chloride on PSAC-N is the highest, which indicates strong ability for acetylene hydrochlorination. The reaction mechanism is determined, and the reaction energy of N-6v(7) calculated as 236.2 kJ mol⁻¹.

Introduction

Polyvinylchloride (PVC), one of the most widely used plastics in the world, has attracted significant research attention because of its diverse range of excellent properties.^[1] For it to replace classical materials, such as wood, iron, copper, and rubber, PVC must meet the requirements of various large-scale application environments. The mercury catalyst (i.e., mercury chloride supported on carbon) plays an important role in producing vinyl chloride monomers through acetylene hydrochlorination.^[2] Unfortunately, the mercury catalyst is highly toxic and causes serious environmental problems. To produce 10³ kg of PVC, approximately 0.12–0.20 kg of mercury is needed.^[3,4] Concerns regarding the use of mercury catalysts for acetylene hydrochlorination have prompted scientists to continue the search for possible alternatives to these catalysts.^[5–7]

Noble-metal catalysts (e.g., gold,^[8,9] palladium,^[10,11] and platinum^[12]) demonstrate stable catalytic activity and high acetylene conversion. However, these catalysts are significantly limited in application because of their low stability and short life, and the use of such catalysts for acetylene hydrochlorination is restricted. Moreover, noble-metal catalysts easily lead to changes in valence state, catalyst aggregation, and deactivation.^[13] Although noble-metal catalysts can satisfy current needs, research to meet the practical requirements remains an

urgent necessity. Thus, the development of low cost, environmentally benign, sustainable non-mercury catalysts, particularly in response to the increasing needs of modern society and emerging ecological concerns, is an important endeavor.

In our previous experiment (Table 1), activated carbon demonstrated reaction activity for acetylene hydrochlorination. Such a finding has prompted us to consider whether a nonme-

Table 1. Conversion of acetylene and selectivity of vinyl chloride with various catalysts after 5 h.^[a]

Sample	X_A [%]	S_{VCM} [%]
coal-based AC	13.24	99.35
PSAC	16.77	99.35
coconut AC	4.65	99.46
SiO ₂	0.32	–
Al ₂ O ₃	0.52	–
TiO ₂	0.29	–

[a] Reaction conditions: $T = 423$ K, $\text{GHSV}(\text{C}_2\text{H}_2) = 36$ h⁻¹, $V(\text{HCl})/V(\text{C}_2\text{H}_2) = 1.15$.

tal catalyst for acetylene hydrochlorination could be obtained. We synthesized a highly active pitch-based spherical activated carbon (PSAC) modified through a nitrogen-doping treatment and evaluated its adsorption behavior by computational analysis (i.e., a Gaussian model). The nitrogen-doped PSAC (PSAC-N) demonstrated high catalytic activity and acetylene conversion. Compared with mercury and noble-metal catalysts, PSAC-N appears to be a promising nonmetal catalyst. By eliminating the effect of trace metals and pore structure, we confirmed that the C–N structure is the active site of PSAC-N. The C–N optimization model was ascertained by computational analysis, and the reaction mechanism of acetylene hydrochlorination with the C–N catalyst was studied by using DFT calculations per-

[a] Dr. X. Wang
School of Chemical Engineering and Technology
Tianjin University
Tianjin 300072 (P.R. China)

[b] Dr. X. Wang, Prof. B. Dai, Y. Wang, Dr. F. Yu
Key Laboratory for Green Processing of Chemical Engineering of Xinjiang
Bingtuan
School of Chemistry and Chemical Engineering
Shihezi University
Shihezi 832003 (P.R. China)

Supporting information for this article is available on the WWW under <http://dx.doi.org/10.1002/cctc.201402018>.

formed with the Gaussian 09 program package. PSAC-N demonstrated superior performance, cost-effectiveness, and environmental safety.

Results and Discussion

Catalytic behavior of carbon and oxide-based catalyst support materials

As shown in Table 1, acetylene conversion was calculated and estimated using carbon and oxide-based catalyst support materials [e.g., activated carbon (AC), SiO₂, Al₂O₃, and TiO₂]. Acetylene conversion induced by AC is higher than that induced by oxide-based catalyst supports. PSAC demonstrated a high catalytic efficiency and acetylene conversion was up to 16.8%, whereas all other oxide-based catalyst supports demonstrated fairly low catalytic efficiency. Moreover, all the carbonic materials, such as PSAC, demonstrated excellent selectivity toward vinyl chloride, which could strongly improve acetylene hydrochlorination. Therefore, PSAC is used as a catalyst and not just as a catalyst support.

Active site distribution of PSAC as a catalyst for acetylene hydrochlorination

To determine the active site distribution of PSAC, nitrogen-doped carbon (NC), trace elements, and the microstructure of PSAC were investigated after PSAC activation. As shown in Figure 1a, nitrogen-doped PSAC (PSAC-N) demonstrated high acetylene conversion. The acetylene conversion rate increased with the increase in NC content. The as-obtained PSAC-N(0.8) sample, which had a nitrogen content of 4.9% (Table 2), demonstrated excellent acetylene conversion (66%). However, PSAC with a nitrogen content of 0.7% demonstrated a low level of acetylene conversion (16.8%). These results indicate that the nitrogen content in PSAC and PSAC-N can improve the acetylene hydrochlorination rate of the catalyst and demonstrate high catalyst activity.

As shown in Figure 1b, acetylene conversion (from 54 to 92%) on PSAC-N(0.8) is high [$T=250^{\circ}\text{C}$; feed volume ratio $V(\text{HCl})/V(\text{C}_2\text{H}_2)=1.15$] at various gas hourly space velocities (GHSVs), ranging from 30 to 150 h⁻¹. To optimize catalyst activity, the GHSV(C₂H₂) must be 120 h⁻¹. The reaction temperature of acetylene hydrochlorination with the PSAC-N(0.8) catalyst was varied from 120 to 300 °C. As shown in Figure 1c, the conversion of acetylene on PSAC-N(0.8) increases with the increase in temperature. If the temperature is 250 °C, the increase in acetylene conversion is slow. Thus, a suitable reaction temperature for the PSAC-N(0.8) catalyst is 250 °C and the acetylene conversion achieved was 68%. Thus, PSAC-N appears to be an appropriate catalyst for acetylene hydrochlorination. Even after 160 h (Figure S1), the acetylene conversion on the PSAC-N(0.8) catalyst remained 58% [$T=250^{\circ}\text{C}$, $\text{GHSV}(\text{C}_2\text{H}_2)=120\text{ h}^{-1}$, $V(\text{HCl})/V(\text{C}_2\text{H}_2)=1.15$].

In addition to the NC content, we studied the microstructure and trace elements of PSAC. The BET results (Table 3) revealed that the specific surface area and the pore volume of coconut

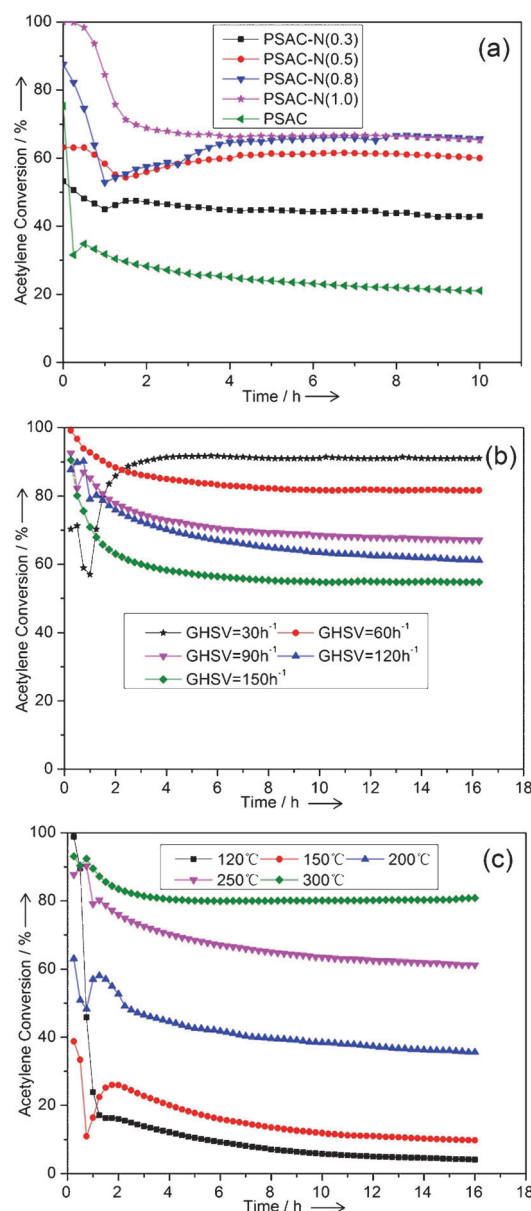


Figure 1. Acetylene conversion of a) various samples at a temperature of 150 °C, a GHSV(C₂H₂) of 36 h⁻¹, and a feed volume ratio $V(\text{HCl})/V(\text{C}_2\text{H}_2)$ of 1.15; b) the PSAC-N(0.8) sample at a temperature of 250 °C and a feed volume ratio $V(\text{HCl})/V(\text{C}_2\text{H}_2)$ of 1.15; c) the PSAC-N(0.8) sample at a GHSV(C₂H₂) of 120 h⁻¹ and a feed volume ratio $V(\text{HCl})/V(\text{C}_2\text{H}_2)$ of 1.15.

Table 2. Elemental contents of the as-obtained PSAC and PSAC-N(X) samples.

Sample	Elemental content [at %]		
	C	N	Others
PSAC	94.40	0.73	4.87
PSAC-N(0.3)	93.99	1.61	4.40
PSAC-N(0.5)	93.97	2.05	3.98
PSAC-N(0.8)	89.14	4.93	5.93
PSAC-N(1.0)	88.59	5.04	6.37

AC were larger than those of PSAC; the corresponding XRD patterns and SEM and TEM images are shown in Figures S2

Sample	BET surface area [m ² g ⁻¹]	Total pore volume [m ³ g ⁻¹]	Adsorption average pore width [Å]
AC	1776.3	1.16	26.1
PSAC	1097.8	0.55	19.9
PSAC-N(0.3)	1006.0	0.55	21.7
PSAC-N(0.5)	941.4	0.51	21.8
PSAC-N(0.8)	935.7	0.53	22.5
PSAC-N(0.8) (after reaction)	872.2	0.49	22.6
PSAC-N(1.0)	928.6	0.51	21.9

and S3, respectively. However, under the reaction conditions [$T=150\text{ }^{\circ}\text{C}$, $\text{GHSV}(\text{C}_2\text{H}_2)=30\text{ h}^{-1}$, $V(\text{HCl})/V(\text{C}_2\text{H}_2)=1.15$], acetylene conversion over PSAC was higher than that over AC, which means that PSAC demonstrated higher catalytic activity than did AC. The conversion of acetylene and selectivity of vinyl chloride over PSAC were 16.8 and 99.3%, respectively. This phenomenon was mainly attributed to NC in PSAC (0.7 wt% of nitrogen).

The X-ray fluorescence technique was used to analyze trace metal elements in the catalysts, and the results are summarized in Table S1. The main contents of PSAC include Ca, Fe, Al, Ba, Zn, K, Cu, and Na elements. We designed an experiment in which CaCl_2 , FeCl_2 , AlCl_3 , BaCl_2 , ZnCl_2 , KCl , CuCl_2 , and NaCl were added at a certain mass ratio (i.e., 0.5%) to PSAC; the as-obtained samples were labeled as PSAC-Ca, PSAC-Fe, PSAC-Al, PSAC-Ba, PSAC-Zn, PSAC-K, PSAC-Cu, and PSAC-Na, respectively. The addition of trace elements was not beneficial to improving acetylene conversion (Figure S4). X-ray photoelectron spectroscopy (XPS) analysis revealed that the contents of Cu in AC and PSAC are similar, which means that Cu species in the AC catalyst are not the active sites.

Inactivation of PSAC-N catalysts

After the completion of the acetylene hydrochlorination reaction, the surface area of the PSAC-N(0.8) catalyst decreased (Table 3). The end gas was absorbed by the 1-methyl-2-pyrrolidinone solution and the solution then subjected to GC-MS for composition analysis. The possible byproducts are dichloroethane, vinyl acetylene, and divinyl acetylene (Figure S5 and Table S2). The decrease in the BET surface area after the reaction indicated that the reason

for inactivation should be acetylene polymerization, which gives rise to carbon deposition and pore blocking.

Adsorption behavior of the catalysts with various NC structures for acetylene hydrochlorination

The XPS analysis of the as-obtained samples was performed to examine the carbon and nitrogen states; and the results are presented in Figure 2. The distinct peak at a binding energy of 248.4 eV was observed in the high-resolution spectrum of C 1s. It is apparent that binding energies of N-5 (nitrogen atom bonded in 5-membered rings) and N-Q (quaternary N bonded among three 6-membered rings) species are determined to be 400.2 and 404.9 eV, respectively.^[14-16] Notably, N-6v (quaternary nitrogen bonded between two 6-membered rings) was observed at 398.6 eV for PSAC, which suggests that N-6v should be one of the active sites for acetylene hydrochlorination.

To confirm the active site of NC in PSAC, the structures of various nitrogen species in AC was built by using the Gaussian model, and the results are presented in Scheme 1. According to the XPS results, the model for PSAC-N is only for N-5, N-Q, N-6v, and N-6 (pyridinic nitrogen, nitrogen atoms bonded in 6-membered rings) structures. The DFT model for N-6v(7) was also built to verify the N-6v model. The adsorption energies were calculated, and the results are summarized in Table S3. The hydrogen chloride adsorptions onto all kinds of NC structures were stable owing to the low adsorption energies. The acetylene adsorption energies onto N-6v and N-6 species are much lower than those onto N-5 and N-Q species, which means that acetylene was apt for adsorption onto N-6v and N-

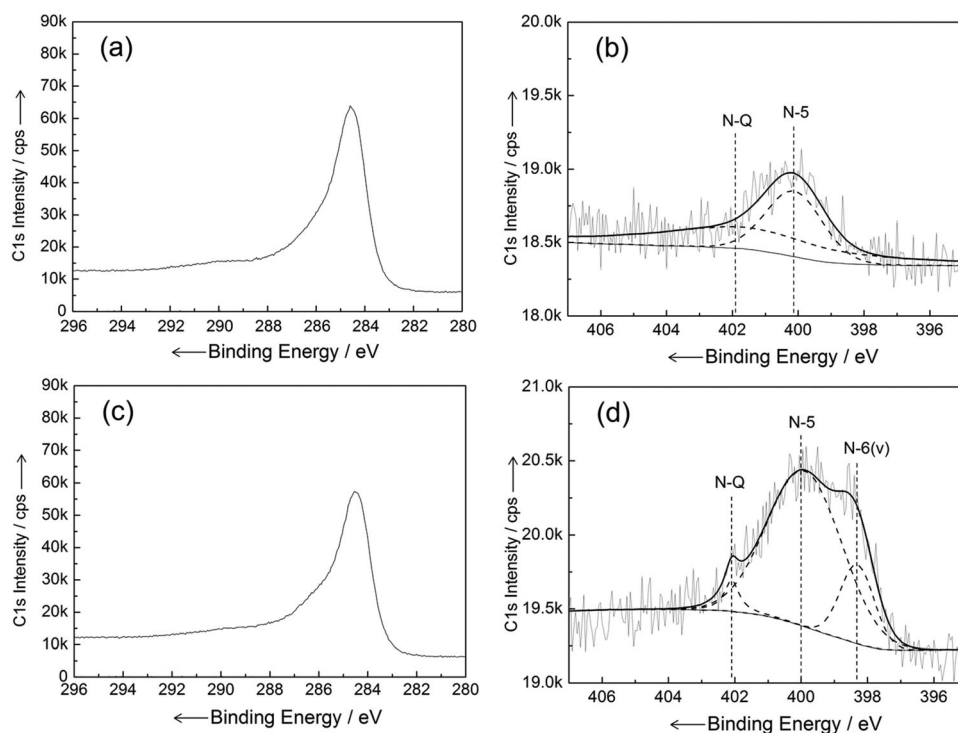
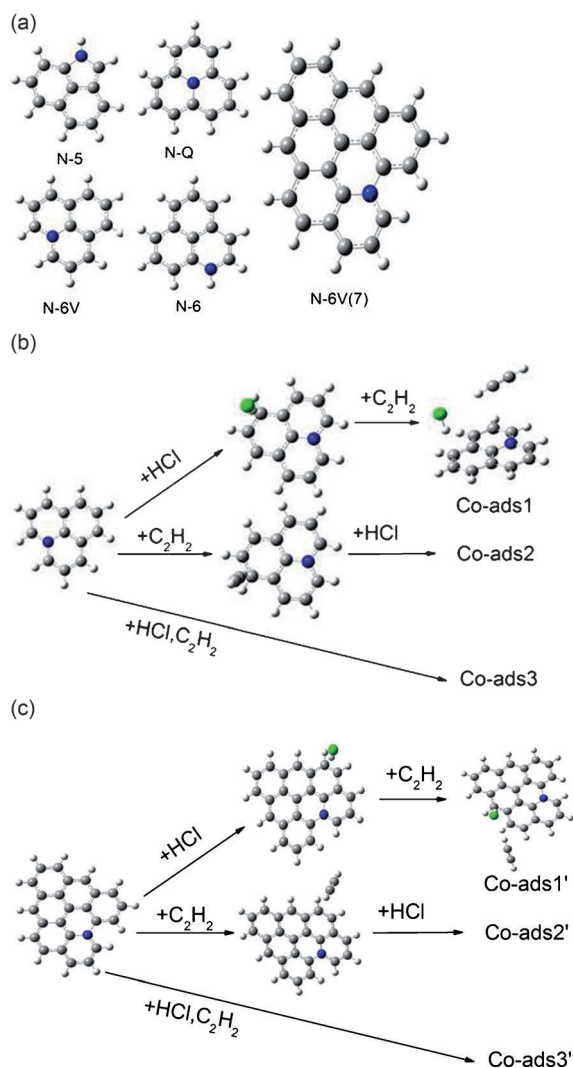


Figure 2. XPS patterns of PSAC and PSAC-N(0.8): a) C 1s for PSAC, b) N 1s for PSAC, c) C 1s for PSAC-N(0.8), and d) N 1s for PSAC-N(0.8).



Scheme 1. a) Structures of N atoms in PSAC. b, c) Adsorption course of acetylene hydrochlorination: three benzene ring unit model N-6V (b) and seven benzene ring unit model N-6V(7) (c). ●: Cl, ●: C, ●: N, ○: H atoms.

6 species. Notably, the vinyl chloride adsorption energy is higher than the acetylene adsorption energy onto N-6v (or N-6v(7)) whereas the vinyl chloride adsorption energy is lower than the acetylene adsorption energy onto N-6 (or N-6v(7)). The temperature-programmed desorption (TPD) results for the PSAC and PSAC-N(0.8) catalysts with hydrogen chloride and acetylene (Figure 3) suggested that the adsorption capacity increased after nitrogen doping, and these results agree well with those of the calculation model.

Theoretically, the reaction materials must be adsorbed before the chemical reaction can proceed. To understand the adsorption mechanism of hydrogen chloride and acetylene over the PSAC catalyst for acetylene hydrochlorination, a schematic illustration is proposed in Scheme 1. The three possible processes are as follows: 1) hydrogen chloride is first adsorbed onto PSAC and then on acetylene; 2) acetylene is first adsorbed onto PSAC and then on hydrogen chloride; and 3) both hydrogen chloride and acetylene are adsorbed at the same

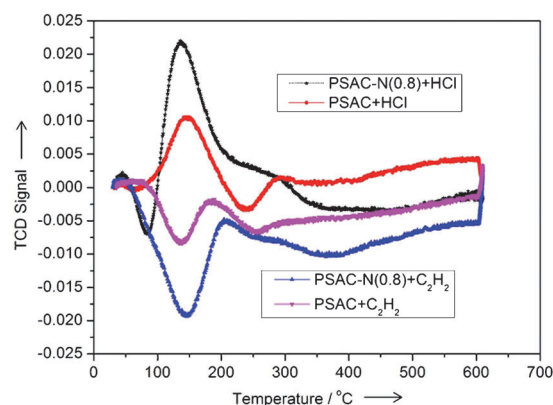


Figure 3. TPD results of PSAC and PSAC-N(0.8) with HCl and C₂H₂. TCD = Thermal conductivity detector.

time. The adsorption results reveal that hydrogen chloride and acetylene are adsorbed in the same site and hydrogen chloride has a lower adsorption energy. The only possible mechanism here for both N-6v and N-6v(7) is that first hydrogen chloride is adsorbed and then acetylene, which forms co-ads1 and co-ads1'. The hydrogen chloride–acetylene complex forms the coordination structure co-ads1 (or co-ads1') with N-6v (or N-6v(7)) (Scheme 1), and the reaction occurs as shown in Figure 3. The structure of co-ads1 (or co-ads1') can convert into co-ads2 (or co-ads2') via transition states TS1 (41.0 kJ mol⁻¹) (or TS1': 23.4 kJ mol⁻¹) and TS2 (166.0 kJ mol⁻¹) (or TS1': 236.2 kJ mol⁻¹), which has a 6-membered ring structure. Finally, vinyl chloride desorbs from PSAC-N. The results presented in Table S3 and Figure 4 revealed that the N-6v and N-6 V(7) models follow the same route in adsorption and reaction, which indicates that the calculation is applicable.

Conclusions

A highly active nitrogen-doped pitch-based spherical activated carbon catalyst (PSAC-N) is prepared through a nitrogen-doping treatment. The optimal reaction conditions are as follows: $T = 250^{\circ}\text{C}$, gas hourly space velocity(C₂H₂) = 120 h⁻¹, and feed volume ratio $V(\text{HCl})/V(\text{C}_2\text{H}_2) = 1.15$. Under these conditions, the corresponding conversion of acetylene is more than 68%. The results reveal that PSAC-N could be a highly active catalyst for acetylene hydrochlorination. The BET, X-ray fluorescence, X-ray photoelectron spectroscopy, GC-MS, and Gaussian calculation results indicate that the nitrogen position has a distinct effect on the rate of acetylene hydrochlorination. The analysis of products and the catalyst before and after the reaction shows that the reason of inactivation is acetylene polymerization. Because hydrogen chloride and acetylene are adsorbed in the same site and hydrogen chloride adsorption energy is lower, first hydrogen chloride must be adsorbed and then acetylene to form co-ads1. The reaction energy of acetylene hydrochlorination over PSAC-N (N-6V(7) structure) is 236.2 kJ mol⁻¹. All results from DFT calculations indicate that acetylene conversion may be increased by increasing the amount of N-6V structures on the PSAC-N catalyst.

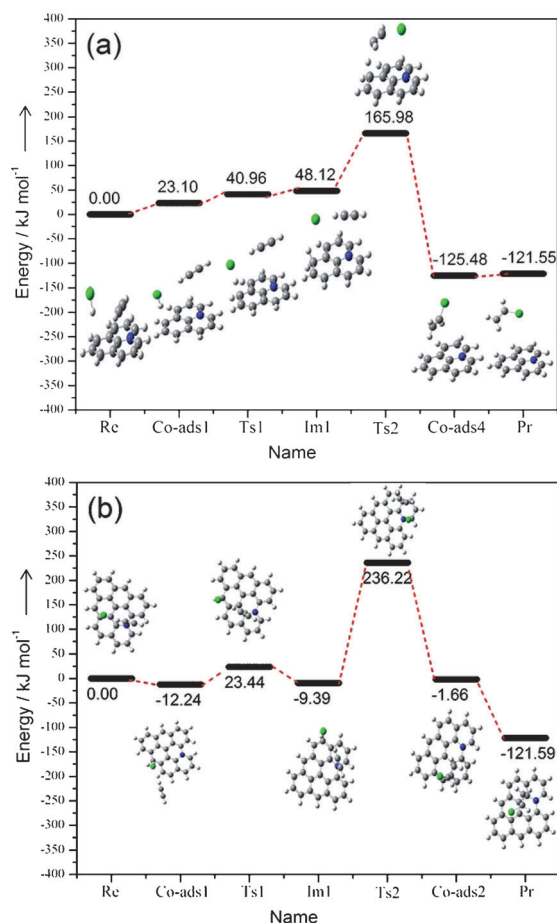


Figure 4. DFT-calculated surface energies for C₂H₂ hydrochlorination: a) three benzene ring unit model N-6V; b) seven benzene ring unit model N-6V(7). ●: Cl, ●: C, ●: N, and ○: H atoms.

Experimental Section

PSAC (20–40 mesh) was washed with dilute aqueous hydrogen chloride (1 mol·L⁻¹) at 70 °C for 5 h to remove Na, Fe, and Cu contaminants, which were poisons for the hydrochlorination reaction.^[8,17] PSAC and melamine were fully mixed at weight ratios of 1:x (x = 0.3, 0.5, 0.8, 1.0), dried at 200 °C for 10 h, and then sintered at 900 °C for 30 min.^[15,18] Finally, the mixtures were boiled for 1 h to obtain the PSAC-N(0.3), PSAC-N(0.5), PSAC-N(0.8), and PSAC-N(1.0) samples.

Activity tests were performed in a fixed-bed microreactor (diameter = 10 mm). The temperature of the reactor was regulated with a CKW-1100 temperature controller (Chaoyang Automation Instrument Factory, Beijing, P.R. China). The experimental setup used herein was identical to that used in our previous study.^[7,8,19] The pipeline was purged with nitrogen before the reaction to remove water and air from the system. Acetylene (10 mL min⁻¹) and hydrogen chloride (11.5 mL min⁻¹) were then fed to a heated reactor containing the catalyst (5 mL) through a filter to remove trace impurities with calibrated mass flow controllers, which gave a GHSV-(C₂H₂) of 120 h⁻¹. The pressure of the reactants was in the range of 0.11–0.12 MPa; the pressure was selected both for safety reasons and for testing the catalyst under mild conditions. The volume speed of the exit gas was similar to the volume speed of acetylene gas. The exit gas mixture was passed through an absorption bottle

containing sodium hydroxide solution and then subjected to GC (Shimadzu GC-2014C) for analysis.^[7,8]

All DFT calculations were performed with the Gaussian 09 program package.^[20] No geometric constraints were assumed in the geometry optimization. The standard 6-311G + ** basis set was used for hydrogen, carbon, nitrogen, and chlorine atoms. Atomic charges were calculated by using the Mulliken-type charges. The frequencies of all the geometries were calculated at the same level to identify the nature of the stationary points and obtain the zero-point-energy corrections. All stationary points were characterized as minima (no imaginary frequencies) or transition state (one imaginary frequency) by using Hessian calculations.^[21,22] Intrinsic reaction coordinate calculations were used to determine that each transition state links the correct product with the reactant.

The specific surface areas and pore distribution of the catalysts were analyzed with an ASAP 2020C surface area and porosity analyzer (Micromeritics Instrument Corporation, USA). Degassing was performed for 6 h at 423 K and then the as-obtained samples analyzed by using liquid nitrogen adsorption–desorption at 77 K. The elemental contents of the catalyst were measured with a Vario EL III element analyzer (Germany). The XPS analysis was performed with a Kratos AMICUS spectrometer equipped with a standard AlK_α X-ray source (300 W) and a pass energy analyzer (20 eV). The X-ray fluorescence analysis was performed with a PANalytical's Venus 200 spectrometer. TPD was also analyzed with an AutoChem 2720 instrument (Micromeritics Instrument Corporation, USA). The samples were pretreated in hydrogen chloride or acetylene atmosphere at the reaction temperature (180 °C) for 4 h and then high-purity nitrogen (50 mL min⁻¹) was passed through the sample at 50 °C for 30 min. The sample was heated from 50 to 650 °C (heating rate: 10 K min⁻¹) to collect the data.

Acknowledgements

This work was supported by the National Basic Research Program of China (973 Program, no. 2012CB720302) and the Program for Changjiang Scholars and Innovative Research Team in University (no. IRT1161).

Keywords: activated carbon · heterogeneous catalysis · hydrochlorination · nitrogen · reaction mechanisms

- [1] X. B. Wei, H. B. Shi, W. Z. Qian, G. H. Luo, Y. Jin, F. Wei, *Ind. Eng. Chem. Res.* **2009**, *48*, 128–133.
- [2] X. Qin, Y. H. Song, R. Jin, J. Shi, Z. Y. Yu, S. K. Cao, *Green Chem.* **2011**, *13*, 1495–1498.
- [3] N. Pirrone, S. Cinnirella, X. Feng, R. B. Finkelman, H. R. Friedli, J. Leaner, R. Mason, A. B. Mukherjee, G. B. Stracher, D. G. Streets, K. Telmer, *Atmos. Chem. Phys.* **2010**, *10*, 5951–5964.
- [4] B. Nkosi, N. J. Coville, G. J. Hutchings, *Appl. Catal.* **1988**, *43*, 33–39.
- [5] M. Conte, A. F. Carley, G. Attard, A. A. Herzing, C. J. Kiely, G. J. Hutchings, *J. Catal.* **2008**, *257*, 190–198.
- [6] G. J. Hutchings, D. T. Grady, *Appl. Catal.* **1985**, *17*, 155–160.
- [7] H. Y. Zhang, B. Dai, X. G. Wang, W. Li, Y. Han, J. J. Gu, J. L. Zhang, *Green Chem.* **2013**, *15*, 829–836.
- [8] H. Y. Zhang, B. Dai, X. G. Wang, L. L. Xu, M. Y. Zhu, *J. Ind. Eng. Chem.* **2012**, *18*, 49–54.
- [9] J. L. Zhang, Z. H. He, W. Li, Y. Han, *RSC Adv.* **2012**, *2*, 4814–4821.
- [10] S. A. Mitchenko, T. V. Krasnyakova, R. S. Mitchenko, A. N. Korduban, *J. Mol. Catal. A* **2007**, *275*, 101–108.
- [11] S. A. Mitchenko, T. V. Krasnyakova, I. V. Zhikharev, *Kinet. Catal.* **2009**, *50*, 734–740.

- [12] K. Zhou, J. C. Jia, X. G. Li, X. D. Pang, C. H. Li, J. Zhou, G. H. Luo, F. Wei, *Fuel Process. Technol.* **2013**, *108*, 12–18.
- [13] M. Conte, A. F. Carley, G. J. Hutchings, *Catal. Lett.* **2008**, *124*, 165–167.
- [14] D. Long, J. Zhang, J. Yang, Z. Hu, G. Cheng, X. Liu, R. Zhang, L. Zhan, W. Qiao, L. Ling, *Carbon* **2008**, *46*, 1259–1262.
- [15] E. Raymundo-Piñero, D. Cazorla-Amorós, A. Linares-Solano, J. Find, U. Wild, R. Schlögl, *Carbon* **2002**, *40*, 597–608.
- [16] M. a. Pérez-Cadenas, C. Moreno-Castilla, F. Carrasco-Marín, A. n. F. Pérez-Cadenas, *Langmuir* **2009**, *25*, 466–470.
- [17] M. Conte, A. F. Carley, C. Heirene, D. J. Willock, P. Johnston, A. A. Herzog, C. J. Kiely, G. J. Hutchings, *J. Catal.* **2007**, *250*, 231–239.
- [18] H. F. Gorgulho, F. Gonçalves, M. F. R. Pereira, J. L. Figueiredo, *Carbon* **2009**, *47*, 2032–2039.
- [19] X. Y. Li, M. Y. Zhu, B. Dai, *Appl. Catal. B* **2013**, *142*, 234–240.
- [20] Gaussian 09, Revision C.01, G. W. T. M. J. Frisch, H. B. Schlegel, M. A. Scuseria, M. A. Robb, J. R. Cheeseman, V. G. Zakrzewski, J. A. Montgomery, R. E. Stratmann, J. C. Burant, et al., Gaussian, Inc., Wallingford CT, **2010**.
- [21] H. B. S. C. Gonzalez, *J. Phys. Chem. C* **1990**, *94*, 5523–5527.
- [22] L. Kang, M. Zhu, Y. Su, S. Zhang, B. Dai, *Can. J. Chem.* **2013**, *6*, 120–125.

Received: February 6, 2014

Revised: March 4, 2014

Published online on July 23, 2014